inter·noise 2004
Prague • Czech Republic • August 22–25

The 33rd International Congress and Exposition
on Noise Control Engineering

Numerical Computation of the Impulsive Sound Generated by a Projectile Discharging from a Muzzle

Jonghoon Bin[a], Jaeheon Kim[b] and Soogab Lee[a*,c]

[a,a*]Center for Environmental Noise and Vibration Research (CENVR), BD 301-1214, Seoul National University, Seoul, Korea
[b]Technical Venture T.F.T, R&D Division, Hyundai Motor Company , Korea
[c]School of Mechanical and Aerospace Eng., Seoul National University, Seoul, Korea

[a]mrbin@snu.ac.kr; [b]cacique@hyundai-motor.com;
[a*,c]solee@plaza.snu.ac.kr

Abstract [338] The goal of this paper is to suggest the numerical method for the simulation of impulsive sound generation and to investigate the acoustic field produced by a projectile discharging from a muzzle. For this problem, a direct simulation using the conventional flow computation method is performed to obtain the acoustic source information in near-field. Computed unsteady flow results are used to obtain the solutions in far-field. Hybrid method using the flow results computed in near-field boundary region combined with an integral formulation to evaluate the radiated noise in far-field is suggested. First, a numerical study on wave dynamic procedure occurring in muzzle flows, which are made by a supersonic projectile released from the open end of a tube into ambient air condition, is implemented. From numerical simulation in near-field, such complex phenomena, including blast waves, jet flows, shock waves and their interactions in the muzzle blast, are described. Second, the Euler equations assuming axi-symmetric flows, which are able to ensure the non-linear effects while propagating outward and to simulate the near/far-field acoustic propagation, are applied for impulsive sound propagation resulting from complex muzzle blast through the unsteady flow results computed above. This numerical method is efficient and powerful computation tool to extend impulsive sound prediction near-field to the very far-field.

1 INTRODUCTION

A variety of military gun propulsion systems have been investigated and developed including those that utilize advanced solid propellant configurations[1,2]. Upon ignition and burning, the solid propellant in these systems takes on a highly complex structure that includes the dynamics of propellant combustion and various multiphase flow phenomena. The numerical study of such aeroacoustic problems places stringent demands on the choice of a computational algorithm, because it requires the ability to propagate disturbances of small amplitude and short waves. The demands are particularly high when shock waves are involved, because the chosen algorithm must also resolve discontinuities in the solution with a stiff source. The extent to which a high-order-accurate shock capturing method in multiphase reacting flows can be relied upon for aeroacoustics applications that involve the interaction of shocks with other waves has not been previously quantified[3,4]. The numerical methodology in obtaining a globally high-order-accurate solution in

such a case with a shock-capturing method is demonstrated through the study of a simplified model problem.

The objective of current study is to develop a numerical technique for noise prediction generated through muzzle blast and to evaluate the utility of computational models in the design of large-scale propellant systems. Especially, it is required to develop a numerical technique with minimum errors of dispersion and dissipation for aeroacoustic applications such as muzzle blast with a supersonic projectile. A direct application of classical DRP(dispersion-relation-preserving) methodology[5] to the finite volume formulation in case of simulation of unsteady base flow in computational region is difficult since DRP scheme with the central differencing approach tries to model spatial derivatives as accurately as possible. Especially, the proposed approach must guarantee highly interacting complex flow information such as muzzle blast and propulsion. As the first stage of all processes, the accurate unsteady base flow is computed in use of high-order dispersion relation based CFD methodology briefly introduced in Section 2.2. The current simulations correctly capture both the levels and nonlinear characteristics of the discontinuous acoustic signals.

Section 2 represents technical approaches to obtain the unsteady base flow results with highly interacting complex flow phenomena. In Section 3, numerical simulation in near-field is implemented with proposed numerical methodology to get unsteady base flow and numerical computation in far-field is carried out by using the computed results in Section 2.

2 TECHNICAL APPROACHES

2.1 Governing Equations

The governing equations are written in two dimensions for the sake of simplicity. Assuming that the effects of viscosity and chemical reaction in the present study are negligible, a dimensionless conservation form of the unsteady Euler equations of a perfect gas can be written in this form.

$$\frac{\partial Q}{\partial t}+\frac{\partial F}{\partial x}+\frac{\partial G}{\partial y}+\frac{S}{r}=0 \tag{1}$$

The conservative flow variable vector Q, the source term vector S and the flux vectors in the streamwise and radial directions, F and G, are given by

$$Q=\begin{pmatrix}\rho\\ \rho u\\ \rho v\\ \rho e\end{pmatrix},\qquad F=\begin{pmatrix}\rho u\\ \rho u^2+p\\ \rho uv\\ (e+p)u\end{pmatrix},\qquad G=\begin{pmatrix}\rho v\\ \rho uv\\ \rho v^2+p\\ (e+p)v\end{pmatrix},\qquad S=\begin{pmatrix}\rho v\\ \rho uv\\ \rho v^2\\ (e+p)v\end{pmatrix} \tag{2}$$

where primitive variables in the vector Q are density ρ, velocity components u and v, the fluid pressure p, respectively. The total energy per unit volume, e, is given by

$$e=p/(\gamma-1)+\tfrac{\rho}{2}(u^2+v^2) \tag{3}$$

In the current implementation, these equations are solved in generalized cartesian coordinates in conservative form to treat the moving boundary of projectile moving body.

2.2 Spatial Discretization

In these equations, flux vector splitting is utilized with the use of numerical approach suggested in previous paper[6]. In order to achieve high spatial accuracy in a finite volume scheme, high-order interpolation formulas for each component of the vector Q_j are used as follows.

$$\widetilde{Q}_{j+1/2}^{L,op} = \sum_{k=1}^{3} w_{L,k}\widetilde{Q}_{j+1/2}^{L,k}$$
$$\widetilde{Q}_{j-1/2}^{R,op} = \sum_{k=1}^{3} w_{R,k}\widetilde{Q}_{j-1/2}^{R,k} \qquad (where, \sum_{k=1}^{3} w_{L,k} = \sum_{k=1}^{3} w_{R,k} = 1) \tag{4}$$

where $w_{L(R),k}(k = 1,2,3)$ and variables at cell interface, $Q_{j-1/2}^{L(R),op}$, are the weighting coefficients and a linear combination of function $Q_{j-1/2}^{L(R),k}$ to be more than fourth-order accurate, respectively. All coefficients are determined on condition that the dispersion relation is maintained in all space and for all time.

Taking the Fourier transform of both sides of Eq.(4) yields

$$\widetilde{Q}(\alpha) = \frac{1}{2\pi}\int_{-\infty}^{\infty} Q(x)e^{-i\alpha x}d\alpha \tag{5}$$

$$Q(x) = \int_{-\infty}^{\infty} \widetilde{Q}(\alpha)e^{i\alpha x}dx \tag{6}$$

$$\widetilde{Q}(\alpha\Delta x) \cong \frac{1}{\Delta x}\left[\sum_{k=1}^{3} w_k e^{i\alpha(\Delta_k)\Delta x}\right], \quad \Delta_k \in \{\cdots \ -5/2 \ \ -3/2 \ \ -1/2 \ \ 1/2 \ \ 3/2 \ \ 5/2 \ \ \cdots\} \tag{7}$$

It is desirable to ensure that the Fourier transform of the finite difference is a good approximation to the partial derivative over the range of wave numbers of interest. Therefore such purpose can be achieved by minimizing the integrated error E, defined by the following:

$$E = \int_0^{\sigma_r} \left|\overline{\alpha}_r\Delta x - \alpha\Delta x\right|^2 d(\alpha\Delta x) + \lambda\int_0^{\sigma_i} \left|\overline{\alpha}_i\Delta x + Sgn(c)\exp\left[-\ln 2\cdot\left(\frac{\alpha\Delta x - \pi}{\sigma}\right)^2\right]\right|^2 d(\alpha\Delta x) \tag{8}$$

As a result, the coefficients used in obtaining unsteady flow results are constructed to minimize the truncation error in the wavenumber space with less grid points per wavenumber and biased stencils for discontinuities. For the simulation of impulsive sound generation and propagation, the base flow values computed here are combined with acoustic perturbation equations to show acoustic source characteristics and sound propagation.

2.3 Dual-Time-Stepping Algorithm

In order to treat the moving boundary of projectile moving body in muzzle, a dual time stepping algorithm is used in the current research. This algorithm was introduced by Jameson[7] for calculations of unsteady flows past airfoils and wings.

To carry out the iterations at each physical time step, an artificial time term, τ, is introduced like this.

$$\frac{\partial Q}{\partial \tau} + \frac{\partial Q}{\partial t} + \frac{\partial F}{\partial x} + \frac{\partial G}{\partial y} + \frac{S}{r} = 0 \tag{9}$$

It is possible to treat the discretization in space and time separately by re-writing Eq.(9) as

$$\frac{\partial Q}{\partial \tau} = -\left(\frac{\partial Q}{\partial t} + R(Q)\right) = -\hat{R}(Q) \tag{10}$$

where $R(Q)$ is the residual which includes the convective and the source fluxes. Once the artificial steady state is reached, the derivative of Q with respect to τ becomes zero, and the original unsteady Euler Equations are recovered. Therefore, instead of solving each time step in the physical time domain, the problem is transformed into a sequence of steady-state computations in the artificial time domain.

In the current implementation, the time derivatives with respect to the physical time, t, are discretized with a three-point backward differencing formula. This results in an implicit linear multi-step method that is second-order accurate in time.

Descretizing Eq.(10) with first order finite difference for artificial time and second order backward difference for the physical time terms results in

$$\frac{Q_p^{k+1} - Q_p^k}{\Delta\tau} + \frac{3Q^{k+1} - 4Q^n + Q^{n-1}}{2\Delta t} + R(Q^{k+1}) = 0 \tag{11}$$

Here, k is the pseudo-iteration number, n is the physical time step number and $R(Q)$ denotes the residual vector, respectively.

2.4 Description of Initial and Moving Boundary Condition

The properties of the gas at the muzzle can be obtained by using the Rankine-Hugoniot relations under the assumption that the gas velocity is equal to the projectile launch speed. Schmidt et al[2] carried out their theoretical analysis based on this assumption and have shown that the obtained results agreed well with experiments. Considering of the friction between the projectile object and the shock tube wall, we simplify initial conditions for numerical simulations as follows. In the initial stage, with the projectile moving down the shock tube, the precursor shock wave is considered as having arrived at the exit of the shock tube and the projectile object is located behind the precursor shock wave at a certain distance that is determined with the projectile release time.

The ambient condition outside of the shock tube is ambient air at $p_{air} = 1 \text{and} T_{air} = 297K$. Behind the precursor shock wave, the properties of gas on either side of the projectile and the projectile itself all move at the same velocity, i.e., the post-shock velocity, V_p. Using the assumption of the projectile speed and the ambient air condition, the initial flow condition between the precursor shock wave and the projectile can be determined using adiabatic shock relations. For the initial flow state behind the projectile body, it is assumed that the friction force acting on the projectile body is proportional to the projectile surface area in contact with the tube wall and the driving force acting on the projectile body is sufficient to overcome the friction and drag force to keep the projectile move at a constant speed while the projectile is moving inside the shock tube. The friction in nature may vary case by case in experiments, but this assumption denotes the fact that the bigger friction force will induce stronger second blast waves. According to the assumption, the state behind the projectile can be calculated from the pressure, p_b, by using the Poisson's adiabatic equation for a perfect gas providing that the gas behind the projectile body is compressed adiabatically from the gas state in front of the projectile to the pressure, p_b. The pressure behind the projectile, p_b, will be taken as 1.5 p_s, where p_s is the post-shock pressure ahead of the projectile.

In order to simulate a moving projectile, it is assumed that the projectile is moving in the fixed main mesh system so that the moving boundary conditions consistent with the Euler equations can be applied on the surfaces of the projectile. At each time step, the mirror-image flow values within the boundary are determined according to the moving surface with the moving speed of V_p.

$$\rho_{in} = \rho_{out}, \;\; p_{in} = p_{out}, \;\; u_{in} = 2 \times V_p - u_{out}, \;\; v_{in} = v_{out} \tag{12}$$

Here, $\rho_{in}, u_{in}, v_{in}$ and p_{in} denote the values within the boundary whereas $\rho_{out}, u_{out}, v_{out}$ and p_{out} represent the values in the flow field. This results in the surface of the projectile behaving like a moving solid wall. Three-columns of interpolated boundary are used to ensure accuracy of the numerical scheme.

Nonreflecting boundary conditions are applied at the inflow, outflow and upper boundaries to minimize effects of nonphysical wave reflection nearby the boundary. Axi-symmetric boundary

condition is applied at lower boundary. Numerical simulations are carried out on an equally spaced grid of 600×250 mesh points. The inner diameter of the shock tube is regarded as a reference length and 50 mesh points are used along the radius for all of the cases.

3 NUMERICAL RESULTS

3.1 Validation of Numerical Results

The first case treated is for the diffraction of a shock wave discharged from a shock tube into air for a shock Mach number of M=2.4 and its computational domain is similar to the present study but without a projectile. The figures show the experimental result[8] on the left in *Figure 1* and the numerical one on the right in *Figure 1*. It can be seen from the comparison that the agreement between computational and experimental results is good.

a. experimental results b. numerical results

Figure 1: *shadowgraph of the first precursor flowfield taken immediately after precursor flow ejection*

3.2 Numerical Simulation of Wave Dynamics in Near-field

In order to compute the near field flow a compressible finite volume unsteady Euler solver is used mentioned earlier. The code uses an implicit solver in time with approximate factorization and dual time stepping method for physical timestep, and is high-order accurate in space through the use of biased upwind differencing with dispersion relation.

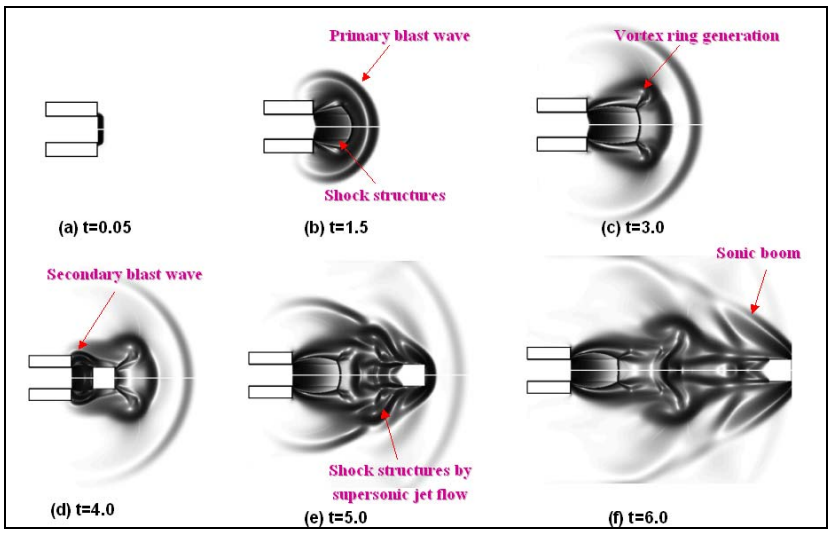

Figure 2: *The density distribution of the muzzle blast at the projectile speed of M=2.0*

Using the same algorithm described earlier[6], we have simulated the impulsive wave dynamics in a propellant muzzle system numerically. *Figure 2* shows the instantaneous density contour of a projectile Mach number 2.0. From the contour, we observe the impulsive first and second blast waves propagating omni-directionally and complex waves propagating on lateral direction. By the interaction between the projectile moving body and the complex shock structures resulting from under-expanded jet phenomena, there exist density fluctuations and impulsive sound waves generated by the interaction of shock, rigid body and spherical vortex.

In muzzle blast problems, acoustic field and large-scale flow field must be solved simultaneously to resolve interaction between shock and vortex or acoustic waves in near field. This high order numerical approach can guarantee the propagation of acoustic variables in the far-field as well as implement large scale interaction between shocks and acoustic waves. In this figure, it is obvious that the numerical technique represents muzzle flow phenomena such as primary blast wave, shock structure and jet core flow in the near field. As mentioned above, this methodology ensures the small scale acoustic wave and flow/acoustic interaction. Therefore, it is reliable that the results in the far field will represent impulsive sounds.

3.3 Numerical Simulation of Impulsive Wave in Far-field

Hybrid method with the flowfield computed in near-field is used to evaluate the far-field impulsive sounds. High-order and high-resolution numerical schemes are applied to the present computation in a structured grid system. Explicit DRP(dispersion-relation-preserving) finite difference scheme[9] is used for evaluating the flux derivatives and an optimized four-step Adams-Bashforth method is used for integrating the governing equations in time. The nonlinear artificial dissipation model by Jameson is also used to remove unwanted numerical oscillations. Radiation boundary conditions[10] are used in the present computation and incoming boundary condition in matching region which is based on incoming and outgoing wave characteristics is used as shown in *Figure 3*. Incoming wave characteristics are given by previous nearfield computations. Inner domain shows the source region in near-field whereas outer domain shows the propagation region in far-field at instantaneous given time.

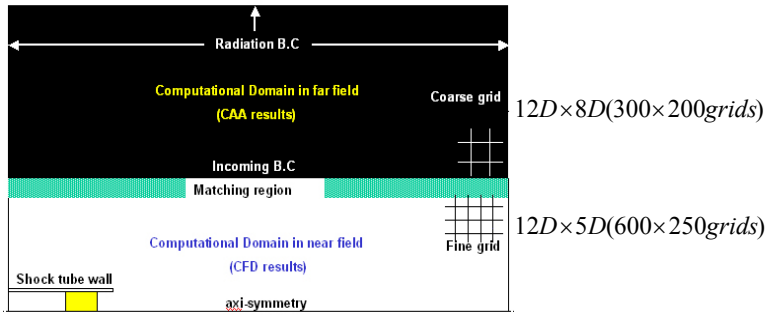

Figure 3: *Computational domain and boundary conditions in near- and far- field*

Impulsive sound waves are also simulated with the help of the computational aeroacoustics(CAA) scheme. The source information calculated in this process can be used to predict the sound pressure levels in the far-field with combining acoustic perturbation equations with non-linear terms.

Figure 4 shows the comparison between the results of near-field compuatation with dispersion relation based CFD method[6] and those of far-field computation with CAA method. In this figure, there are good agreements between the pressure contours, especially same propagation speed in

matching region. As a result, this hybrid methodology can guarantee the propagation of acoustic variables in the far-field as well as implement large scale interactions between shocks and waves. Particularly, it can be easily combined with traditional RANS, LES or DNS to identify acoustic sources in near field.

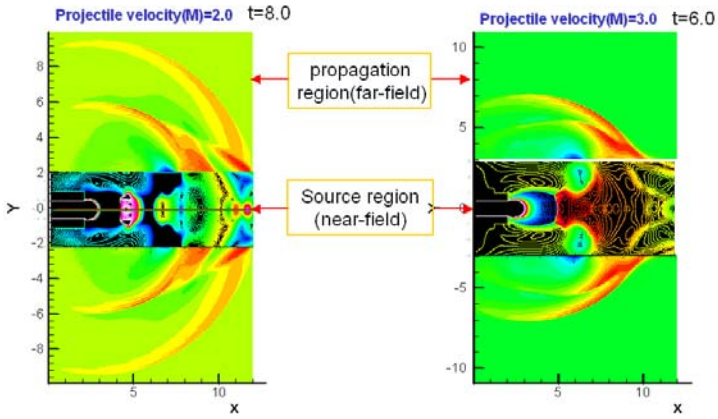

Figure 4: *Comparison between the results of farfield compuatation with CAA method and those of nearfield computation with CFD*

And so, it has the potential to make significant impact on aeroacoustics research and development such as impulsive sound generation and propagation problems.

4 CONCLUSION

In this paper a highly effective numerical technique has been developed for simulating multi-scale aeroacoustic problems where impulsive sound is generated or nonlinear effects are dominant. This hybrid methodology can guarantee the propagation of acoustic variables in the far-field as well as implement large scale interaction between shocks and waves. The numerical technique has been validated through several problems and applied in muzzle blast problems with projectile speed, i.e., M=2. This method can be easily combined with traditional RANS, LES or DNS to identify acoustic sources in near field. Therefore, it has the potential to make significant impact on aeroacoustics research and development such as impulsive sound generation and propagation problems. Further research is to apply them to 2- and 3- dimensional Euler/Navier-stokes equations for accurate noise prediction of muzzle blast.

ACKNOWLEDGEMENTS

This work was supported by the International Cooperation Research Program of the Ministry of Science & Technology and by grant No.R01-2001-000-00401-0 from Korea Science & Engineering Foundation.

REFERENCES

[1] E.M. Schmidt, G.D. Kahl, and D.D. Shear, “Gun blast: Its propagation and determination”, *AIAA Paper*, No.80-1060 (1980)

[2] E.M. Schmidt, and D.D. Shear, “The formation and decay of impulsive, supersonic jets”, *AIAA Paper* 74-531 (1974)

[3] San-Yih Lin and Jeu-Jiun Hu, “Parametric Study of Weighted Essentially Nonoscillatory Schemes for Computational Aeroacoustics”, *AIAA Journal*, **39**, No.3 (2001)

[4] Xiaogang Deng and Hanxin Zhang, "Developing High-Order Weighted Compact Nonlinear Schemes", *Journal of Computational Physics*, **165**, 22-44 (2000)
[5] C.K.W. Tam, "Computational aeroacoustics: issues and methods", *AIAA Journal,* **33**, 1788(1995)
[6] J.Bin, C.W.Lim, C.Cheong and S.Lee, "A Numerical Technique for the Simulation of Impulsive Noise Generation and Propagation", *The 32nd International Congress and Exposition on Noise Control Engineering*, Seogwipo, Korea, August, 25-28, (2003)
[7] A.Jameson, "Time dependent calculation using multi-grid, with applications to unsteady flows past airfoils and wings", *AIAA Paper 91-1596, AIAA 10th Computational Fluid Dynamics Conference*, (1991)
[8] "Gun muzzle blast and flash", *Progress in Astronautics and Aeronautics*, **Vol.139**, AIAA
[9] C.K.W. Tam and J.C.Webb, "Dispersion-Relation-Preserving Finite Difference Schemes for Computational Acoustics", *Journal of Computational Physics,* **107**, 262 (1993)
[10] C.K.W. Tam, Z. Dong, "Radiation and Outflow Boundary Conditions for Direct Computation of Acoustic and Flow Disturbances in a Nonuniform Mean Flow", *Journal of Computational Acoustics*, **4** (2) 175-201 (1996)
[11] National Aeronautics and Space Administration, Glenn Research Center, "Third Computational Aeroacoustics (CAA) Workshop on Benchmark Problems", August (2000)